Lowest Energy Structures of Gold Nanoclusters

I. L. Garzón,[1] K. Michaelian,[1] M. R. Beltrán,[2] A. Posada-Amarillas,[3] P. Ordejón,[4] E. Artacho,[5]
D. Sánchez-Portal,[5] and J. M. Soler[5]

[1]*Instituto de Física, Universidad Nacional Autónoma de México, Apartado Postal 20-364, Mexico, D.F., 01000 Mexico*
[2]*Instituto de Investigaciones en Materiales, Universidad Nacional Autónoma de México, Apartado Postal 70-360, Mexico, D.F., 04510 Mexico*
[3]*Centro de Investigación en Física, Universidad de Sonora, Apartado Postal 5-088, Hermosillo, Sonora, 83000, Mexico*
[4]*Departamento de Física, Universidad de Oviedo, Calle Calvo Sotelo s/n, 33007, Oviedo, Spain*
[5]*Departamento de Física de la Materia Condensada C-III, Universidad Autónoma de Madrid, 28049 Madrid, Spain*

(Received 13 March 1998)

The lowest energy structures of Au_n ($n = 38, 55, 75$) nanoclusters are obtained by unconstrained dynamical and genetic-symbiotic optimization methods, using a Gupta n-body potential. A set of amorphous structures, nearly degenerate in energy, are found as the most stable configurations. Some crystalline or quasicrystalline isomers are also minima of the cluster potential energy surface with similar energy. First principles calculations using density functional theory confirm these results and give different electronic properties for the ordered and disordered gold cluster isomers. [S0031-9007(98)06933-6]

PACS numbers: 36.40.Cg, 36.40.Mr, 36.40.Qv, 61.46.+w

Gold nanoclusters are a fundamental part of recently synthesized molecular nanocrystalline materials [1–5]. This is one of the reasons why theoretical and experimental studies on structural, dynamical, electronic, and other physical and chemical properties of isolated and passivated gold clusters, as well as their size dependence, are at the forefront of cluster science [1–8]. A further interest in doing research on these systems is motivated by the convergence of experimental and theoretical methods to study gold clusters in the size range of 1–2 nm. Structural characterization using a variety of experimental techniques can be performed on Au_n nanoclusters of these diameters, corresponding to aggregates with $n = 20$–200 atoms [9,10]. On the theoretical side, computational power is currently available to study Au_n clusters in this size range, using methods going from molecular dynamics (MD) simulations based on semiempirical n-body potentials [6,11] to first-principles calculations using density functional theory (DFT) [12].

Despite the existence of sophisticated experimental and theoretical tools to study gold nanoclusters, several questions on, for example, their structural properties (most stable cluster configuration, lowest-lying isomers, thermal stability, size evolution, etc.) remain unsolved [8,9,11]. Experimentally, a further increase in the resolution of structural probes like x-ray powder diffraction seems to be necessary to decompose the remaining broad features in the structure factors of Au_n clusters [9,10] and obtain a conclusive determination of the structures. Theoretically, several calculations on the structures of gold nanoclusters have been made using fixed cluster symmetries as constraints during a local optimization of the structure [8,9,12]. However, a global, unconstrained minimization of the cluster structures is necessary for an exhaustive search of minima on the potential energy surface (PES) [11]. Additional efforts are thus necessary to elucidate the structural properties of gold nanoclusters and their interplay with other physical (electronic, optical, etc.) properties, fundamental for the design of gold-based nanostructured materials.

In this Letter, we present results on the most stable (lowest energy) configurations of intermediate-size (1–1.5 nm) Au_n ($n = 38, 55, 75$) nanoclusters obtained through dynamical and genetic-symbiotic (evolutive) [13] optimization methods using a Gupta n-body potential [14]. For the three sizes investigated, corresponding to the so-called magic number clusters [15], we did not find as the most stable cluster configuration a single ordered structure with a definite symmetry. Instead, we obtained a set of lowest-lying isomers (minima of the PES), nearly degenerate in energy. Moreover, most of these cluster configurations have no spatial symmetry, and therefore can be classified as amorphouslike or disordered structures. Some crystalline (or quasicrystalline) structures are also found as minima of the PES with similar energies as the disordered clusters. First principles calculations, using DFT in the local density approximation (LDA), confirm the equal stability (degeneracy in energy) of both types of structures. However, the calculated electronic properties of the amorphous and ordered clusters show clear differences in, for example, their electron density of states and their spatial charge distribution.

Our initial approach to determine the lowest energy cluster configurations was based on global optimizations (no assumptions are imposed on the cluster symmetry) using simulated annealing (SA) with MD simulations and a semiempirical n-body potential [11,16]. Simulated quenching (SQ), in which fast cooling rates are applied to the system on selected regions of phase space, where a catchment area of a local minimum is located, increases the efficiency of this dynamical optimization [16].

 0031-9007/98/81(8)/1600(4)$15.00

The n-body interaction modeling the metal cluster bonding is taken from a tight-binding approximation to the second moment of the electron density of states [14]. Specifically, the size-dependent, Gupta n-body potential with parameters fitted simultaneously to bulk and cluster properties [11,16] was used in the MD simulation. The appropriateness of this potential to describe transition and noble metal clusters as well as its similarity with other related potentials (embedded atom method, effective medium theory, glue potential, etc.) has been broadly discussed [17].

When the SA and SQ methods were applied to the optimization of Au_n ($n = 38, 55, 75$) nanoclusters, an interesting trend was observed: A set of nearly degenerate structures was obtained as the lowest-lying isomers. Most of these structures can be classified as amorphous based on the features of their pair distribution functions [18,19]. Even more intriguing, for clusters with $n = 38$ and 55, the lowest energy configurations are amorphous instead of crystalline (O_h) or quasicrystalline (I_h) structures. However, the difference in binding energy per atom between the most stable disordered and the first lowest-lying ordered isomer is smaller than 0.4 meV/atom for Au_{38} and 9.4 meV/atom for Au_{55}. For the $n = 75$ cluster the situation is reversed: the energy difference between the lowest energy isomer with D_h symmetry and the next local minimum with amorphous structure is 5.7 meV/atom.

Figure 1 displays the lowest energy amorphous and ordered cluster structures together with their vibrational density of states (DOS) and the corresponding distribution of pair distances (DPD). The latter show a tendency toward more continuous distributions than the ordered DPD's [see insets in the $n(r)$ curves of Fig. 1] and already have the splitting of the second peak, characteristic of bulk amorphous metals [19]. A similar broadening is observed in the vibrational DOS of the disordered isomers with respect to those of the ordered ones. Thus, it is justified, in analogy with the bulk case, to classify such structures as amorphous clusters.

The structural stability of the amorphous and ordered isomers was tested in several ways: First, the final cluster temperature at which the SA and SQ methods were stopped was extremely low (10^{-9} K). Second, a time propagation through MD simulations of 10^5 steps was applied to each cluster configuration at its corresponding minimum. Relative changes in the atomic positions larger than 10^{-8} were not observed. Finally, a normal mode analysis was done on the lowest energy cluster isomers, which, in turn, gave us the low temperature harmonic vibrational spectra presented in Fig. 1. The entropy effect at finite temperatures was studied through a determination of the cluster free energy using the calculated frequencies. A comparison of the free energy at finite temperatures for amorphous versus crystalline structures shows an enhancement of the stability of the amorphous with respect to the crystalline structures for the three sizes investigated [20].

Two questions remained after the analysis of the above results: Despite the fact that all conceivable symmetric

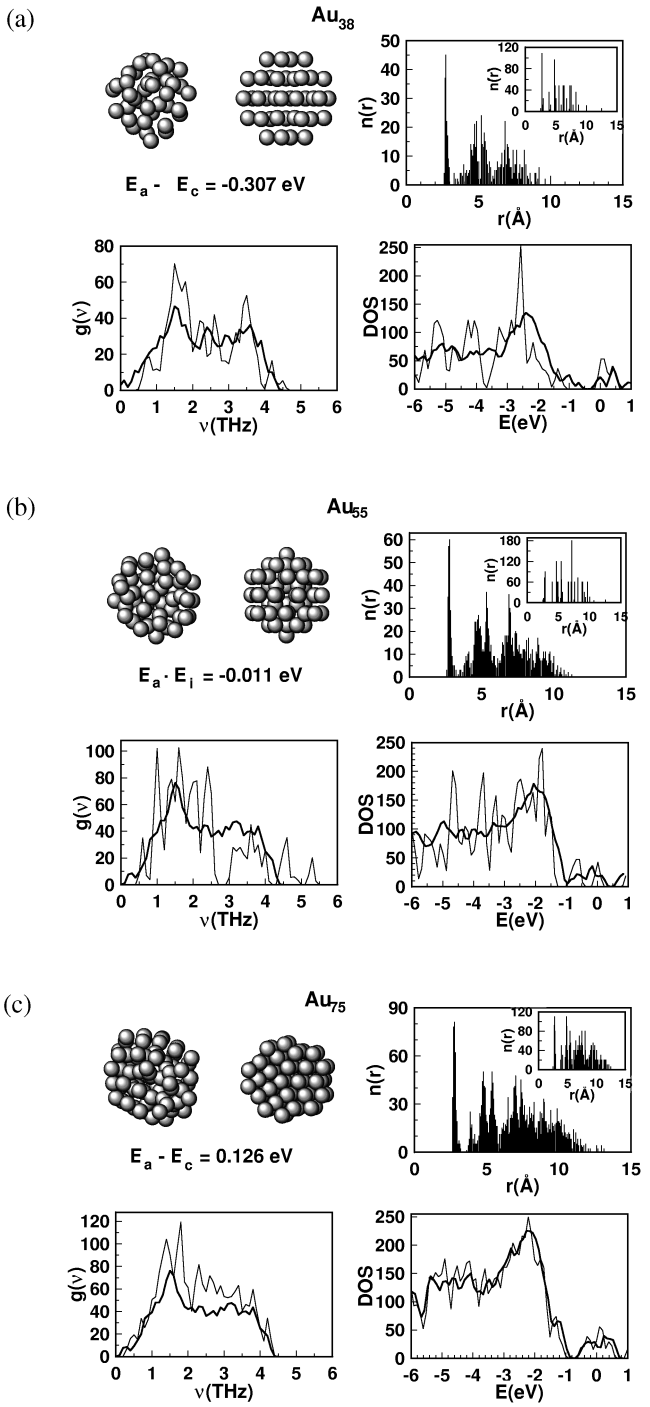

FIG. 1. Cluster structures, distribution of interatomic pair distances [$n(r)$], vibrational density of states [$g(\nu)$], and total electron density of states (DOS) for the lowest energy amorphous and ordered isomers of Au_n ($n = 38, 55, 75$) nanoclusters. The DFT-LDA calculated difference in cluster energy between the lowest energy amorphous isomer and the first ordered structure is shown. Insets on the $n(r)$ curves correspond to the distribution of pair distances of the ordered isomers. The vibrational DOS's were obtained by convoluting the discrete harmonic frequencies with a Gaussian broadening of 0.1 THz. The DOS curves were obtained using a Gaussian broadening of 0.1 eV for the discrete DFT-LDA electron level spectrum (the Fermi level is at 0 eV). Vibrational and electron DOS results for the ordered isomers are also included for comparison (thinner lines).

structures were tested, could other unknown structures still exist with lower energy, but were not found with the SA and SQ methods? Does the n-body Gupta potential provide an adequate description of the PES of gold nanoclusters? The first question is based on the fact that even though SA and SQ methods are robust optimization methods, they do not guarantee the obtainment of the global minimum of the PES, especially for large systems. Since these optimization methods are very time consuming, it is not possible to characterize the complete topography of the PES and thereby gain insight into the cluster dynamical behavior [21].

Evolutive algorithms have been very useful in making extensive searches for lowest energy configurations of clusters with a high efficiency [13,22]. In the present work a version of a symbiotic algorithm together with a conjugate-gradient local refinement [13] was implemented using the n-body Gupta potential to make exhaustive global cluster structure optimizations, to within a relative energy accuracy of 10^{-8}, starting from 70 000 distinct random configurations for clusters of 75 atoms and 50 000 for the other sizes. The results from our evolutive optimizations confirmed the trend described above on the lowest energy structures of the Au_n nanoclusters and provided a complete distribution of their lowest-lying isomers. Many distinct, but almost degenerate in energy, stable configurations were found within a very narrow energy range from the ground state. For example, the 100 lowest energy configurations were found within 6.0, 10.0, and 10.0 meV/atom for the cluster sizes of 38, 55, and 75 atoms, respectively. This region of high density of states contains predominantly amorphous structures for all cluster sizes. For Au_{38}, the ground state is formed by two amorphous units symmetrically located. The second isomer is the fcc crystalline structure followed by other disordered structures. For $n = 55$, the ground state is amorphous, and there are about 80 other amorphous states of lower energy than the I_h icosahedron structure. No other conceivable symmetric structures with lower energy other than the amorphous states mentioned here were found. For Au_{75}, we found the Marks-Dh decahedron [9] and other structures based on it as the most stable followed by a large number of part ordered and part disordered pure amorphous structures.

To understand the physical origin of the amorphous ground states in Au_n clusters we also optimized Ni_n and Ag_n clusters of the same sizes using the n-body Gupta potential. In contrast to Au clusters, the potential parameters of Ni and Ag generate a longer range interaction, which gives raise to a reverse behavior; i.e., symmetric structures for the ground states are preferred and the lowest-lying isomers of higher energy are separated by a finite energy gap from the ground state. In Au nanoclusters, the short-range interatomic interactions between low coordinated and well separated surface atoms generate uncorrelated disordered subunits that form the amorphous structures [11,23].

The coexistence of amorphous and crystalline Au_n nanocluster structures with similar energies predicted by the above semiempirical calculations motivated us to perform a first-principles study of the relative stability of ordered and disordered gold clusters. In this manner, it was possible to test the validity of the predictions given by the n-body Gupta potential and gain insight into the bonding mechanisms and electronic properties of Au_n clusters. DFT-LDA was the chosen technique. The calculations were performed using the SIESTA program [24] to solve the standard Kohn-Sham self-consistent equations in the LDA approximation, using a linear combination of numerical atomic orbitals as the basis set. A nonlocal norm conserving scalar relativistic Troullier-Martins pseudopotential [25] was incorporated so that only the 11 valence electrons per Au atom were considered. Tests of the pseudopotential as well as the size of the basis set were realized on Au_2 and bulk Au. Specifically, 60 Ry in the energy cutoff of the finite real-space grid [24] and single-z s, p, and d orbitals were used to obtain small relative errors (compared to experimental values) in the dimer equilibrium distance (2.4%) and bulk lattice constant (1.3%), with checks up to 100 Ry and a polarized double-z basis. Since a fully *ab initio* MD optimization would be computationally prohibitive, our approach consisted in using the already optimized (through the classical MD and evolutive approaches) cluster structures as initial configurations in an unconstrained conjugate-gradient structural relaxation using the DFT-LDA forces.

The quantum mechanically reoptimized cluster structures obtained through this method were used to calculate their binding energies and electronic properties. The same energy ordering was found for the DFT reoptimized structures and those obtained through the n-body Gupta potential. Our DFT-LDA results indicate that the calculated differences in binding energies per atom between the lowest energy amorphous structures and those with high symmetry are smaller than 0.01 eV/atom for the three sizes investigated, confirming the trend predicted through the semiempirical n-body Gupta potential. The average nearest-neighbor distances, calculated by DFT-LDA in this work, compare very well with those obtained through a scalar relativistic all-electron density functional method [12] for the ordered structures with $n = 38$, 55. For example, for Au_{38} in the O_h symmetry, our calculated average nearest-neighbor distance of 2.77 Å is in excellent agreement with the value of 2.78 Å reported in Ref. [12]. In addition, the calculated difference in binding energy per atom (0.05 eV/atom), between the I_h and O_h isomers with $n = 55$, is very close to the value of 0.06 eV/atom reported in Ref. [12]. This agreement gives additional support to the prediction of equal stability of amorphous and ordered isolated gold nanoclusters obtained in this work and indicates the level of accuracy in our DFT-LDA calculation. Corrections to the DFT-LDA results due to spin polarization effects are expected to be small since gold is a nonmagnetic metal [12]. As well, it is known that the

generalized gradient approximation does not change the relative binding energies of gold isomers with respect to the local density results [12]. Similar results to ours on the equal stability of disordered and ordered isomers of metal clusters have also been found in Pt_{13} using DFT-LDA [26].

Although the disordered and ordered Au_n isomers are very close in energy, their calculated electronic properties are different. Figure 1 shows the total electron DOS for both types of structures. In the amorphous isomers, the electron states are more evenly distributed in energy than those resulting from the ordered structures for the three sizes investigated. This effect is attributed to the break of spatial symmetry in the amorphous clusters. Such an effect could lead to different cluster optical responses according to their size and symmetry [10]. On the other hand, all the clusters studied show a "metallic behavior," independent of their size and structural symmetry. The calculated spatial charge distribution is not only different between the disordered and ordered isomers of a given size but is also size dependent. For the O_h isomer with $n = 38$, the electron charge is slightly greater at the center of the cluster, and the charge of the 6 central atoms sums to $66.1e$, compared with $263.9e$ coming from the 24 surface atoms. In the amorphous cluster a random distribution of electron charge density is observed. For Au_{55} in the I_h configuration, the amount of electron charge oscillates from the center toward the surface, while in the amorphous isomer the charge density is again randomly distributed. However, in Au_{75}, both the ordered and amorphous isomers have a random distribution of electron charge within the whole cluster.

In conclusion, using semiempirical and first principles approaches to describe the bonding in isolated gold nanoclusters and employing unconstrained optimization methods, we have found essentially equal structural stability for amorphous and ordered isomers of Au_n ($n = 38, 55, 75$) clusters with sizes in the range 1–1.5 nm. In addition, the analysis of their calculated distribution of minima (stable configurations) shows a much higher abundance of disordered structures relative to the ordered ones. Preliminary analysis of the local short-range order in the amorphous gold nanoclusters suggests their classification in terms of the relative abundances of very stable structural subunits, based on regular and distorted pentagonal bipyramids [11,20]. Therefore, we expect further experimental efforts in the near future, to confirm the above predictions and provide a complete characterization of gold (amorphous and ordered) nanoclusters. In fact, in recent high resolution electron microscopy studies on Au and Pd nanoparticles, images of polycrystalline and amorphous structures have been reported in the size range of a few nanometers [27,28]. We note that the similar stability of disordered and ordered structures predicted in the present Letter refers to *isolated* gold nanoclusters. At this moment, it is not clear if the effect of the passivation process, necessary during the cluster growth [1], would affect the crystallinity of the resulting sample. Work in such a direction is currently in progress. The possible existence of novel physical and chemical properties of small metal amorphous nanoparticles provide motivation for further theoretical and experimental studies on these systems since they would be useful in the fabrication of new materials based on amorphous nanostructures.

This work was supported by DGSCA-UNAM Supercomputer Center, DGAPA-UNAM under Project No. IN101297, CONACYT, Mexico under Grant No. 25083-E, and Spain's DGES under Grant No. PB95-0202.

[1] R. L. Whetten *et al.,* Adv. Mater. **5**, 8 (1996).
[2] R. P. Andres *et al.,* Science **272**, 1323 (1996).
[3] C. A. Mirkin *et al.,* Nature (London) **382**, 607 (1996).
[4] A. P. Alivisatos *et al.,* Nature (London) **382**, 609 (1996).
[5] R. P. Andres *et al.,* Science **273**, 1690 (1996).
[6] W. D. Luedtke and U. Landman, J. Phys. Chem. **100**, 13 323 (1996).
[7] D. Bethell and D. J. Schiffrin, Nature (London) **382**, 581 (1996).
[8] C. L. Cleveland *et al.,* Z. Phys. D **40**, 503 (1997).
[9] C. L. Cleveland *et al.,* Phys. Rev. Lett. **79**, 1873 (1997).
[10] T. G. Schaaff *et al.,* J. Phys. Chem. **101**, 7885 (1997).
[11] I. L. Garzón and A. Posada-Amarillas, Phys. Rev. B **54**, 11 796 (1996).
[12] O. D. Häberlen *et al.,* J. Chem. Phys. **106**, 5189 (1997).
[13] K. Michaelian, Am. J. Phys. **66**, 231 (1998); Chem. Phys. Lett. (to be published).
[14] V. Rossato, M. Guillope, and B. Legrand, Philos. Mag. A **59**, 321 (1989).
[15] D. J. Wales, Science **271**, 925 (1996).
[16] J. Jellinek and I. L. Garzón, Z. Phys. D **20**, 239 (1991); I. L. Garzón and J. Jellinek, Z. Phys. D **20**, 235 (1991); **26**, 316 (1993).
[17] S. M. Foiles, Mater. Res. Bull. **21**, 24 (1996).
[18] J. P. Rose and R. S. Berry, J. Chem. Phys. **98**, 3262 (1993).
[19] A. Posada-Amarillas and I. L. Garzón, Phys. Rev. B **53**, 8363 (1996).
[20] I. L. Garzón and A. Posada-Amarillas (to be published).
[21] K. D. Ball *et al.,* Science **271**, 963 (1996).
[22] D. M. Deaven and K. M. Ho, Phys. Rev. Lett. **75**, 288 (1995); D. M. Deaven *et al.,* Chem. Phys. Lett. **256**, 195 (1996).
[23] K. Michaelian, N. Rendón, and I. L. Garzón (to be published).
[24] P. Ordejón, E. Artacho, and J. M. Soler, Phys. Rev. B **53**, 10 441 (1996); D. Sánchez-Portal *et al.,* Int. J. Quantum Chem. **65**, 453 (1997).
[25] N. Troullier and J. L. Martins, Phys. Rev. B **43**, 1993 (1991).
[26] S. H. Yang *et al.,* J. Phys. Condens. Matter **9**, L39 (1997).
[27] S. Tehuacanero *et al.,* Acta Metall. Mater. **40**, 1663 (1992).
[28] W. Krakow, M. J. Yacamán, and J. L. Aragón, Phys. Rev. B **49**, 10 591 (1994).